Perovskite Photovoltachromic Supercapacitor With All-Transparent Electrodes

Feichi Zhou, [⊥,†,‡] ***Zhiwei Ren,*** [⊥,§] ***Yuda Zhao,***[†,‡] ***Xinpeng Shen,***[†,‡] ***Aiwu Wang,***[∥] ***Yang Yang Li,*** [∥] ***Charles Surya,***[§] ***and Yang Chai****[*,†,‡]

[†] Department of Applied Physics, The Hong Kong Polytechnic University, Hung Hom, Kowloon, Hong Kong, People's Republic of China.
[*]Corresponding author: ychai@polyu.edu.hk

[‡] The Hong Kong Polytechnic University Shenzhen Research Institute, Shenzhen, People's Republic of China

[§] Department of Electronic and Information Engineering, The Hong Kong Polytechnic University, Hung Hom, Kowloon, Hong Kong, People's Republic of China

[∥] Department of Physics and Materials Science, City University of Hong Kong, 83 Tai Chee Rd., Kowloon, Hong Kong, People's Republic of China

[⊥]These authors contributed equally to this work.

Abstract: Photovoltachromic cells (PVCCs) are of great interest for the self-powered smart windows of architectures and vehicles, which require widely tunable transmittance and automatic color change under photo-stimuli. Organometal halide perovskite possesses high light absorption coefficient and enables thin and semitransparent photovoltaic device. In this work, we demonstrate co-anode and co-cathode photovoltachromic supercapacitors (PVCSs) by vertically integrating a perovskite solar cell (PSC) with MoO_3/Au/MoO_3 transparent electrode and electrochromic supercapacitor. The PVCSs provide a seamless integration of energy harvesting/storage device, automatic and wide color tunability and enhanced photo-stability of PSCs. Compared with conventional PVCC, the counter electrodes

of our PVCSs provide sufficient balance charge, eliminate the necessity of reverse bias for bleaching the device, and realize reasonable *in-situ* energy storage. The color states of PVCSs not only indicate the amount of energy stored and energy consumed in real time, but also enhance the photo-stability of photovoltaic component by preventing its long-time photo-exposure under fully charged state of PVCSs. This work designs PVCS devices for multifunctional smart window applications commonly made of glass.

Keywords: photovoltachromic supercapacitor (PVCS), perovskite solar cell, electrochromic, energy storage, photo-stability

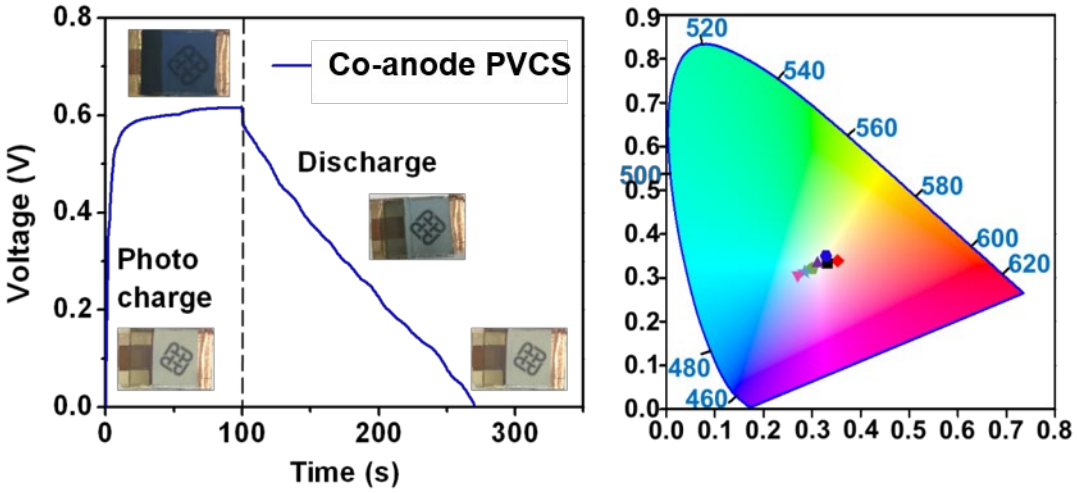

Optically switchable materials have broad applications in the building architectures, vehicle windows, aircrafts, and sunroofs, because they not only reduce cooling/heating costs and ventilation loads, but also enhance the thermal and visual comfort for indoor users.[1-6] Therefore, the smart windows with electrochromic (EC), photoelectrochromic (PECC) and photovoltachromic cells (PVCC) have received increasing attention, where the optical transmittance change can be stimulated and reversed in response to an external stimuli. In the conventional PECC, Pt counter electrode of dye-sensitized solar cells (DSSC) is replaced by WO_3 electrode, where the color change can be driven by photovoltaic potential resulted from optical illumination. Compared with PECC, patterned WO_3/Pt electrochromic electrode are used in PVCC, which can be colored under short-circuit condition, and realize tunable transmittance states and fast responses. [7-10] In these conventional PECC and PVCC devices, the electrochromic materials are typically employed as only one of the electrodes of the device, and their transmittances can fast response to the illumination and switch between the bleached and colored states. However, the energy harvested from the solar cell in these kinds of devices is only used to trigger the change of optical transmittance, and the devices lack of the ability of storing the harvested solar energy because of the limited capacity of the counter electrode (*e.g.,* indium tin oxide) of the capacitor. Thus, the harvested solar energy is not fully used in these kinds of device configurations.

The light sources for photovoltaic devices are usually intermittent and unpredictable. The integration of photovoltaic and energy storage/electrochromic

device together makes it possible to provide sustainable power source and retain the PVCC in a desired colored state. There have been a number of works integrating the photovoltaic cells and energy storage devices (supercapacitor or battery) together to realize a self-powered energy storage device.[11-15] Xu *et al.* demonstrated the integration of perovskite solar cell (PSC) and lithium ion batteries, and reported a high total photoelectric and energy conversion efficiency (~7.8%) and excellent cycling stability.[16] Wang's research group integrated organometallic PSC and polypyrrole-based supercapacitor, and realized a high output voltage of 1.45 V and high energy conversion efficiency of 10%.[17] Integrated smart electrochromic windows for energy storage application have also been studied recently.[18-21] However, these prototypes are connected by two separated energy conversion and storage devices through external wires or power management circuit. This configuration reduces the integration level, causes additional Ohmic loss, and lacks of dynamic solar light control. Subsequently, researchers have made lots of efforts to combine energy conversion and storage functions into one device and improve the integration level. Wee and his co-workers demonstrated a stacked photo-supercapacitor, in which the organic photovoltaics (OPV) and carbon nanotube (CNT) supercapacitor share a common electrode, and the internal resistance of the device is reduced by 43% as well as the power loss.[22]This kind of structure has also been studied for dye-sensitized solar cell (DSSC) integrated with the CNT supercapacitors. [23-25] However, there is still quite few works that report the integration of electrochromic supercapacitor and

semitransparent solar cell into one device, which possesses higher integration level and allows dynamic solar light control.

In this work, we integrate the semitransparent PSC and electrochromic WO_3 supercapacitor into a photovoltachromic supercapacitor (PVCS) in a vertically stacked configuration. Our structures improve the integration level, achieve widely and automatically tunable optical transmittance of the integrated device, and store the electrochemical energy accompanying with the color change. In addition, the electrochromic supercapacitor enhances the photo-stability of PSC by blocking part of the solar light during the fully charged state, which alleviates the photo-degradation issue of the PSC for outdoors application under long-term solar light exposure. This multifunctional PVCS device provides great advantages over conventional smart window design.

Results and discussions

Integration of Co-anode and Co-cathode PVCSs. Figure S1 is a schematic of the fabrication process flow of a PSC by one step method. Figure 1a shows the schematic diagram and photo of a PSC with a MoO_3/Au/MoO_3 (MAM) transparent electrode, which is used for our integrated PVCS structures. The structure of the other PSC part is similar to our previous works.[26] Figure S2a and S2b show the absorption spectra and SEM image of the perovskite thin film. A typical PSC device with Au top electrode exhibits a high efficiency of 16.4%, as shown in the Figure S2c. Here we replace top electrode with a stacked transparent structure, MoO_3 (adjacent to

spirOMeTAD)/Au/MoO_3 (15 nm/12 nm/20 nm), which has been also employed as transparent electrodes in organic photovoltaic cells (OPV) and light emitting diodes (LED).[27-29] The transparent MAM structure shows a transmission of 77.1% at the wavelength of 600 nm and the average visible transmission (AVT) of 70.6% within the wavelength range of 380~780 nm (Figure 1b). The whole PSC device with the MAM top electrode has a higher transmission (>40%) at a longer wavelength above 650 nm (Figure 1c). We demonstrate a typical PSC with the transparent MAM top electrodes, showing good power conversion efficiencies (PCE) of 12.54 % and 9.35 % with the light illuminated from both FTO side and MAM side, respectively, as shown in Figure 1d. This all-transparent-electrode PSC provides photo voltage for the electrochromic part, and allows solar light to be illuminated from both sides.

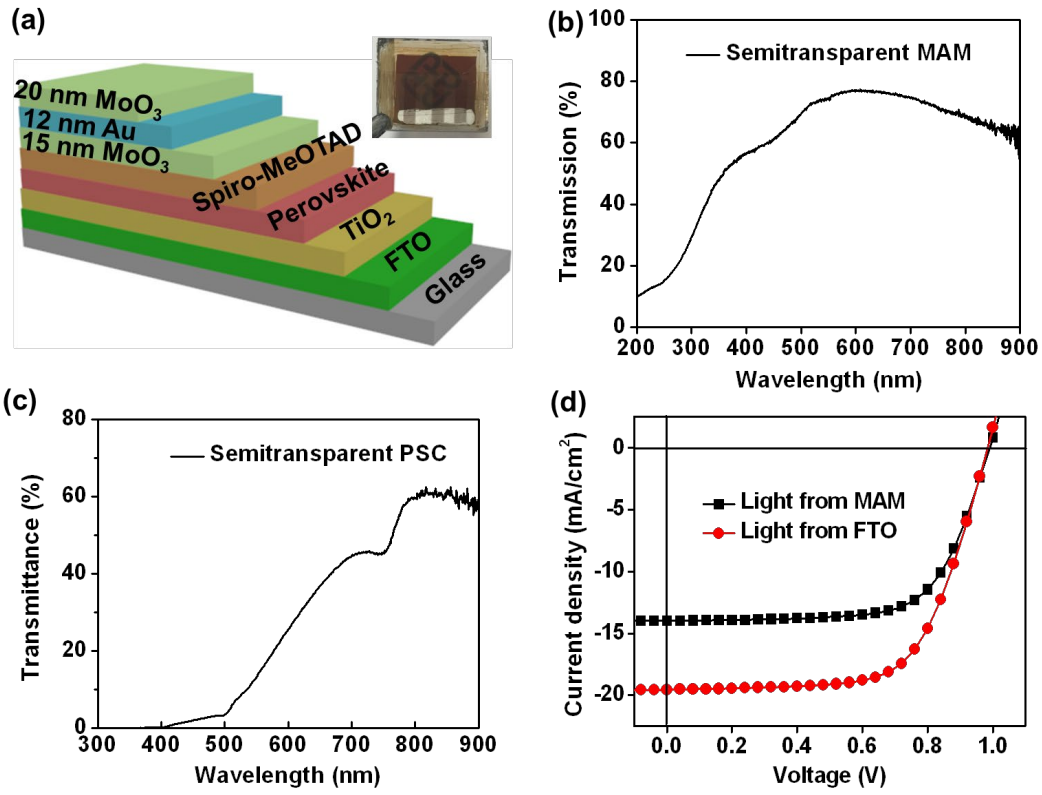

Figure 1. (a) Schematic diagram and photo of PSC with MAM transparent electrode. (b) UV-Vis spectra of the as-fabricated MAM, showing an AVT of 70.6 %. (c) UV-Vis spectra of the whole PSC device with the MAM top electrode. (d) *J-V* curves of a typically semitransparent PSC (MAM electrode) with the light illuminated from both FTO side and MAM side, exhibiting PCEs of 12.54% and 9.35%, respectively.

Both electrochromism and energy storage of WO_3 electrode involve the electrochemical reaction at the interface between electrode and electrolyte, where the valence states of electrochromic WO_3 electrode are changed and lead to energy storage in the meantime. [30-33] The integration of WO_3 based electrochromic device together with PSC enables a new type of PVCC structures.[7] Figure S3 shows characterization results of the WO_3 thin films by thermal evaporation. We further integrate all-transparent-electrode PSC with electrochromic supercapacitor (ECS) in a vertically stacked configuration to form a PVCS, which possesses both wide range for tunable transmittance and seamless integration of energy conversion and storage.

Figure 2a and 2d show the schematic diagrams of the two stacked PVCS structures, namely co-anode structure and co-cathode structure. More detailed structure information is illustrated in three-dimensional and cross-sectional schematic in Figure S4. In the co-anode structure (Figure 2a), a transparent ECS device is integrated and shares an electrode with the semitransparent PSC. The light is illuminated from the top side and transmitted through the ECS cathode to PSC. We fabricated both PSC part and ECS anode on one common glass. The transparent MAM electrode (15 nm/12 nm/20 nm) serves as a co-anode for both PSC and ECS.

We then deposited another 200 nm MoO_3 thin film in the ECS part as the ECS anode to obtain a better capacity. The top WO_3 electrode of the ECS was assembled with the PSC and the ECS anode through the gel-like PVA/H_2SO_4 electrolyte, and works as both the "electrochromic shelter" of the PSC and the cathode of the ECS. This type of PVCS structure avoids of the use of electrical wires during the photo-charging compared with the PVCC designed in Ref. 7. For the co-cathode structure (Figure 2d), a symmetric WO_3 ECS is stacked on the PSC. The PSC and ECS share a glass with both sides coated with FTO, where both sides are electrically connected. The FTO serves as the cathodes for both PSC and ECS. The WO_3 thin film was first deposited on one side of FTO, and the PSC part was fabricated on the other side of the FTO. The WO_3 anode on single-side FTO was then assembled with the above parts through the PVA/H_2SO_4 electrolyte.

Tunable Optical Transmittance of PVCSs. For the integrated co-anode and co-cathode PVCSs, the solar light can illuminate from the side of ECS, and transmit through the ECS device to the PSC. Figure 2a-c and 2d-f schematically show the working mechanisms of the co-anode and co-cathode devices, where the initially charged state, fully charged state and bleached state are illustrated, respectively. For both co-anode and co-cathode PVCSs, the devices were photo-charged under AM 1.5 illumination in the short-circuit condition by connecting terminal A and C. Discharging process was conducted through the external circuit by connecting terminal A and B of the two ECS electrodes, where the discharged current density was controlled as 0.1 mA/cm^2. For the co-anode device, during the photo-charging

process, the electrons and holes are generated in the perovskite layer, and are transported to the electron conducting layer TiO_2 and the hole transport layer Spiro-OMeTAD, respectively. The semitransparent MAM electrode collects holes, which serves as the anode of both ECS and PSC at terminal B. For the co-cathode device, the two FTO cathodes of the PSC and ECS are kept connected at terminal B during the whole charging process and collect the photo-generated electrons. The photovoltaic potential drives the re-distribution of ions in the electrolytes, and the electricity is stored at the WO_3 electrode of the ECS in the form electrochemical energy. Then the charged PVCSs can be discharged through the external circuit by connecting terminal A and B. During the photo-charging process of the two integrated PVCSs, electrons are injected into the WO_3 cathode and H^+ moves towards the ECS anode driven by the electric-field ($WO_3+H^++e \rightarrow HWO_3$). Charges are stored at the WO_3 cathode during the oxidation reaction, and the color changes from transparent to blue, which is accompanied with the chemical state of W changing from 6+ (bleached state) to 5+ (colored state).[34, 35] The other ECS anode works as a charge balancing counter electrode. During the discharging stage, the reversible reduction process releases the charge ($HWO_3 \rightarrow WO_3+H^++e$), and the WO_3 thin film recovers to be transparent, which allows a new working cycle of the integrated device.

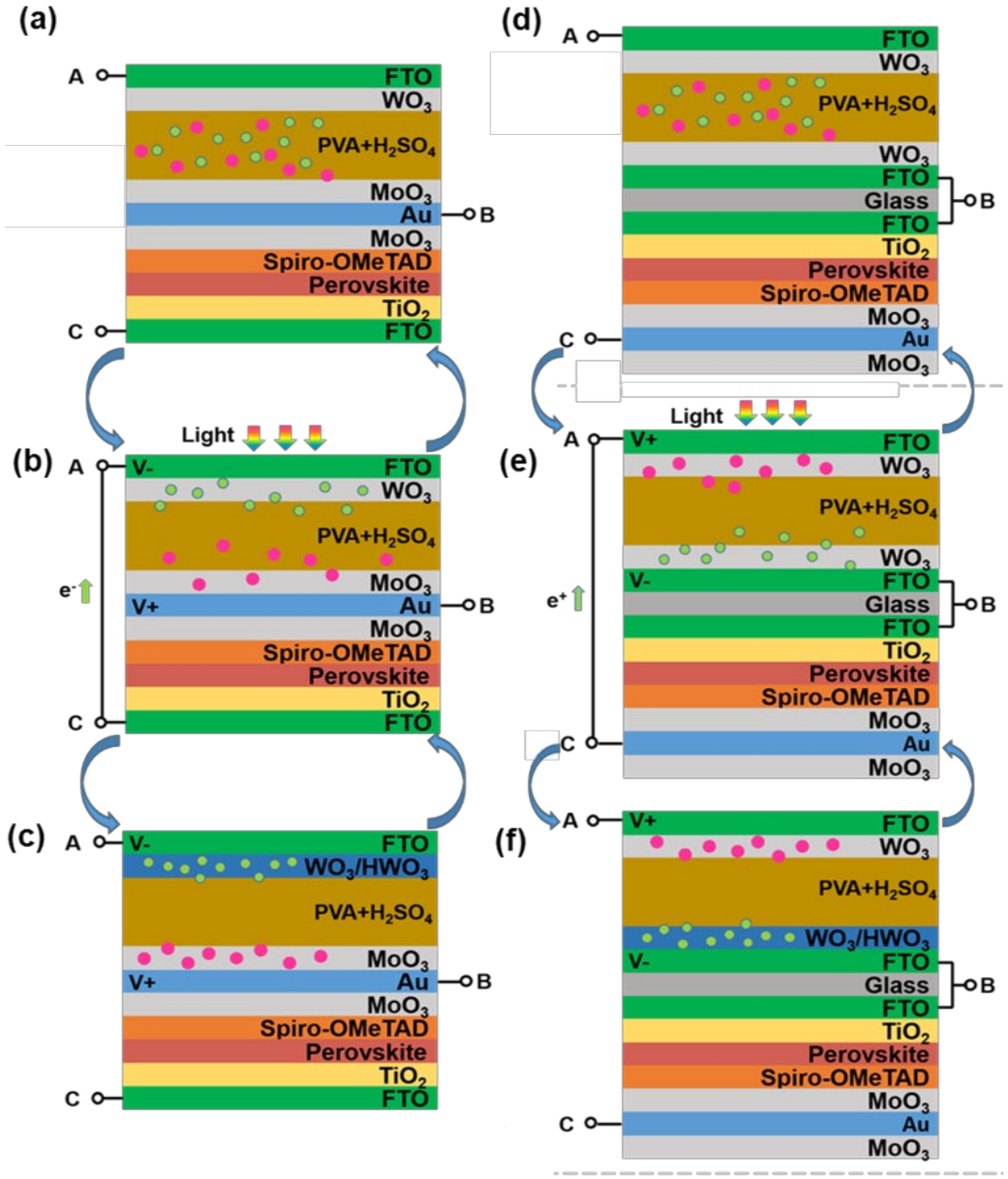

Figure 2. Schematics of co-anode and co-cathode PVCS working mechanism. Original states of (a) co-anode and (d) co-cathode PVCS. At the original states, ECS parts are transparent and at a bleached states, which allow solar light to pass through. Initial charged states of (b) co-anode and (e) co-cathode PVCS: under the solar illumination, electric-fields are formed in the PSC parts which power the ECS. Electrons are injected into the WO_3 cathode, and H^+ moves towards to the WO_3 cathode driven by electric-field. Charges are stored at the WO_3 cathode during the reversible oxidation reaction. The colors are starting to change. (c) and (f) Fully charged states: with the continuous light illumination, the PVCSs reach their fully charged states. The ECS color turns to blue, accompanying with the chemical

state of W charging from 6+ (bleaching state) to 5+ (coloring state). These whole processes are reversible. After the discharging through external circuit, the reversible reduction process releases the charge and the WO_3 thin film recovers to be transparent, thus the PVCSs recover to their bleached states.

Tunable color states can be achieved in our PVCS devices. Figure 3a and 3b show the photos of the co-cathode and co-anode PVCSs under bleached, half charged and fully charged states. The color of the ECS parts turn to deep blue during the photo-charging and recovers to transparent after discharging. We define a 'PSC shelter' here to describe the PVCS working states. The light transmits from the PSC shelter to the PSC. In the co-anode device, the PSC shelter is FTO/WO_3/PVA electrolyte; and in the co-cathode device, the PSC shelter is FTO/WO_3/PVA electrolyte/WO_3/FTO/glass. Figure 3c and 3d demonstrate the transmission spectra of PSC shelters in the two integrated PVCSs corresponding to different colored states. The transmission peaks in blue-purple region are exhibited in the colored PSC shelters, and the other wavelengths in the visible light region are largely reduced. The AVT of co-anode (co-cathode) PVCS is significantly reduced from 76.2% (68.7%) to 54.2% (38.2%) to 35.1% (23.0%) corresponding to the bleached, half charged and fully charged states of the PSC shelters in the PVCSs. Figure 3e demonstrates the color coordinates of the "PSC shelters" with transmission spectra of Figure 3c and 3d under AM 1.5 illumination plotted on the CIE xy 1931 chromaticity diagram. The color coordinates of both bleached PSC shelters lie in the central region in the chromaticity diagram, close to the AM 1.5 illumination. As the PVCSs are kept charging, the PSC

shelters are colored, and there is a shift from central to blue region. However, the coordinate of the colored PSC shelters still locate close to the central region of CIE diagram, demonstrating good color neutrality. This neutrality renders this PVCS with great potential in the building application.

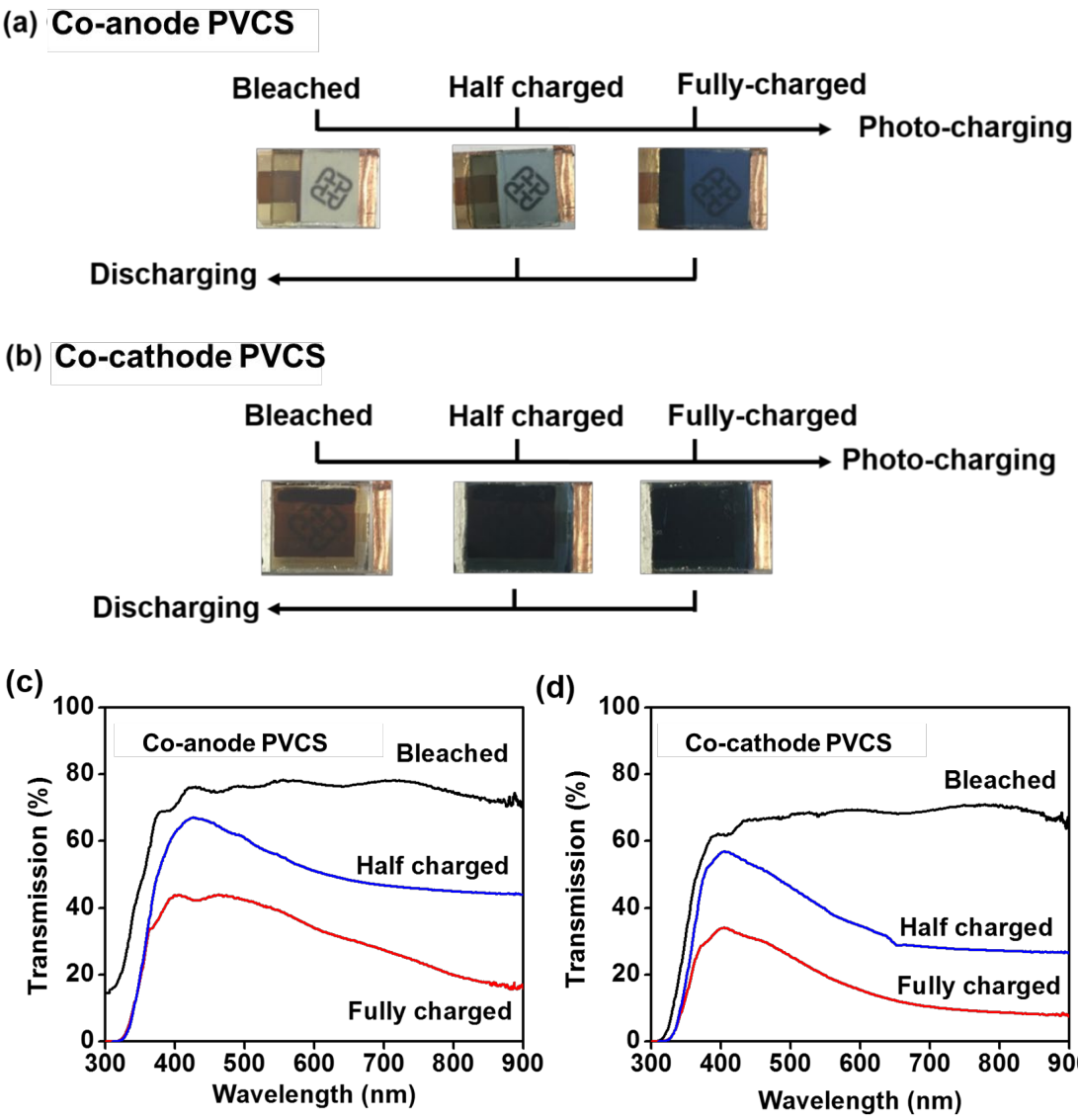

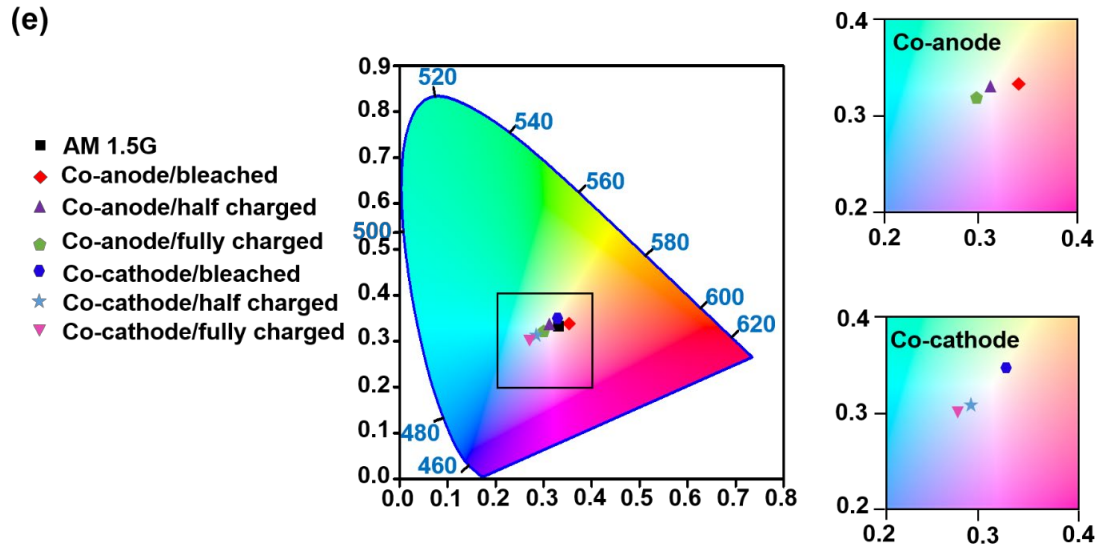

Figure 3. The photos of (a) Co-anode and (b) co-cathode PVCS color states under bleached, half charged and fully charged. Transmission spectra of PSC shelters in (c) co-anode PVCS and (d) co-cathode PVCS corresponding to different color states. Accompanying with energy storage, the color of PSC shelters changes from transparent to blue with a reduction in AVT from 76.2 % (68.7%) to 35.1 (23.0%) for co-anode PVCS and co-cathode PVCS, respectively. (e) Color coordinates of the PSC shelters with transmission spectra of 3(c) and (d) under AM 1.5 illumination plotted on the CIE xy 1931 chromaticity diagram.

***In-situ* Energy Storage of PVCSs.** The tunable color state of the PVCS is also an indicator of the amount of energy stored in the cell, which allows us to estimate the stored energy in PVCS by differentiating its colored state. Figure 4a and 4b show the voltages of the two PVCSs as a function of time evolution during the photo-charging and discharging process**,** and the color states corresponding to the charging and discharging processes. The discharging process was conducted at a constant current density of 0.1 mA/cm^2 by disconnecting terminals A and C (shown in the Figure 2) and no additional solar input will charge the supercapacitor during the discharging process. The co-anode PVCS was charged to 0.61 V within 60 s, and the co-cathode PVCS was charged to 0.68 V within 85 s. For the color change response, the co-anode (co-cathode)

PVCS starts to change its color at a voltage of 0.55 (0.50) V, corresponding to a charging time of 10 s (13 s), and reach a saturated color state until the charging continues for 40 s (56 s). The energy density, average power density and specific areal capacitance of PVCS through photo-charging are calculated as 13.4 (24.5) mWh/m^2, 187.6 (377.0) mW/m^2 and 286.8 (430.7) F/m^2, respectively**,** as documented in Table 1. The energy density of our PVCS is much larger than other types of self-powered energy storage systems, such as pizeo-supercapacitor and triboelectric nanogenerator.[36, 37] The specific areal capacitances of our PVCSs are much larger than those of the graphene-based photo-supercapacitor, [13, 14] the integrated energy fiber based on CNT fiber and Ti wire,[12] and other energy fiber integrating DSSC and electrochemical supercapacitor based on TiO_2 nanotube-modified Ti wire.[19] This is also higher than self-powered smart electrochromic window based on WO_3 supercapacitor.[18] We also integrate the discrete energy harvesting and storage devices through external wires. Figure S5 shows the integration of a PSC with MAM anode and a symmetric WO_3 ECS connected by external wires. The supercapacitor was fully charged to 0.80 V within a 60-70 s light illumination and the discharging process lasted for 400 s at a current density of 0.1 mA/cm^2. The energy density, average power density and areal capacitance of the integrated device are 35.9 mWh/m^2, 461.5 mW/m^2 and 459.6 F/m^2, respectively. The performance is comparable with the device integrating commercial Si solar cell and ECS (Figure S6). However, this configuration with separated PSC and ECS not only reduces the integration level, but also fails to dynamically control the light transmission through the PVCS.

Table 1. Lists of internal resistance, energy density, average power density and areal capacitance of two types of PVCSs. The calculations are according to the discharge curve.

Device Type	Internal resistance (Ω)	Energy density (mWh/m^2)	Power density (mW/m^2)	Areal capacitance (F/m^2)
Co-anode	215	13.4	187.6	286.8
Co-cathode	275	24.5	377.0	430.7

In other types of integrated solar-powered electrochromic windows reported in Ref. 7 and 20, the researchers usually employed the structure of TCO/WO_3/electrolyte/TCO in the ECS part. The TCO counter electrodes have very limited charge storage capability, and cannot provide sufficient balancing charge during the discharging process of the ECS. After the PVCC is converted to the colored state by a positive voltage (V), a reverse bias (-V) is required for converting the PVCC from the colored to the bleaching state. From the typical CV curve of the WO_3/electrolyte/TCO, there is no current response under a voltage scanning from V to 0, unless a reverse bias -V is applied. [7, 20] In contrast, our integrated PVCS devices enable an automatically working cycle of the color change during the charging/discharging process by replacing commonly used TCO anode with MoO_3/WO_3 as a charge balancing counter electrode. An extra reverse bias is not required for converting back to the bleached state, because the MoO_3/WO_3 counter electrode in our PVCS can provide more balancing charge than the ITO electrode in conventional PVCC. Our PVCSs can be bleached by discharging the ECS through external load. After the stored electrochemical energy is consumed, the ECS recovers to be transparent, and a new working cycle can be initiated. This feature can be also confirmed from our cyclic voltammetry (CV) curve and galvanostatic charging/discharging (GCD) curve. [38] Figure 4c and 4d show the CV and GCD curves

of a symmetric WO_3 ECS. Within a voltage scanning range 0-V, a cycle of forward and reverse voltage scanning can realize a color change from bleached state to colored state, and back to the original bleached state. These characteristics provide an automatically working PVCS device for both energy storage and tunable colored states.

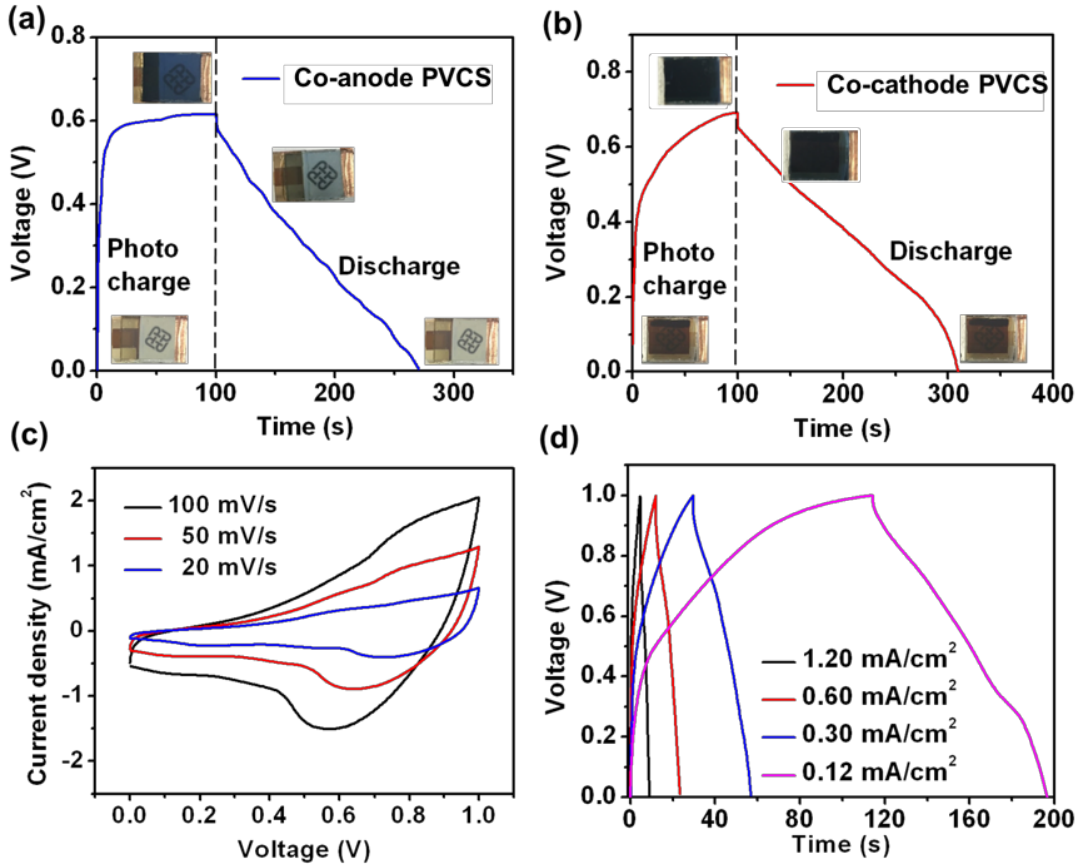

Figure 4. (a) and (b)The V-t curves of the co-anode PVCS and co-cathode devices for the photo-charging process within 100 s and discharging process at a current density of 0.1mA/cm^2.(c) and (d) CV curves and GCD curves of a symmetric WO_3 ECS.

The considerably reduced charging current density can be responsible for a higher energy accumulated. The energy density (24.5 mWh/m^2) and areal capacitance (430.7 F/m^2) of the ECS charged to 0.68 V by PSC in our co-cathode PVCS

configuration are higher than those of discretely symmetric WO_3 ECS (14.8 mWh/m^2 and 119.9 F/m^2) through electrochemical working station, which is charged with a small current density of 0.12 mA/cm^2 to a higher voltage of 1 V (shown in Figure S7). These characteristics can be attributed to the charging way by photovoltaic device. As the light on, the PSC generates the photocurrent within a few seconds, which is considered as the initial charging current (0.4 mA/cm^2) and leads to a fast charging rate. As the supercapacitor is kept charging and colored, the current density supplied by the PSC is significantly reduced. Additionally, as the supercapacitor reaches its fully charged state, the charging current is reduced continuously until the supercapacitor reached saturation. [24, 25] After the supercapacitor is charged to 0.45-0.5 V, there is a significant drop in the charging rate, which suggests a continuously reduced charged current density, thus leading to higher capacitance and energy density accumulated.

Photo-Stability Enhancement of Perovskite Solar Cells. Figure 5a and 5b show the *J-V* curves of the two PSCs utilized in the co-anode and co-cathode PVCSs under different states. We first characterize the performance of the PSCs utilized in the two integrated co-anode and co-cathode PVCSs, respectively. The PSC (PDMS/MAM/spirOMeTAD/perovskite/TiO_2/FTO/Glass) for the co-anode PVCS with the light illumination from the MAM side demonstrates the V_{oc} of 0.983 V, J_{sc} of 12.46 mA/cm^2, fill factor (FF) of 65.4%, and PCE of 8.25%; the PSC (Glass/FTO/TiO_2/perovskite/ spirOMeTAD/MAM) for the co-cathode PVCS with the light illumination from the FTO side exhibits the V_{oc} of 1.000 V, J_{sc} of 18.17 mA/cm^2, FF of 65.4% and PCE of 11.89%, as shown in the Table 2. After the integration with the

transparent ECS, both J_{sc} and PCE of the two PVCSs decrease to about 68% of single PSCs because the ECS has a certain level of light absorption. With the color change of the ECS by photo-charging, J_{sc} are further reduced by about half. The PCE of the co-anode and co-cathode PVCSs drops to 3.73% and 2.26%, respectively. This suggests the PSCs in the PVCSs supply the ECS part in a small current density and are at a low-power working state under the colored state of PVCSs.

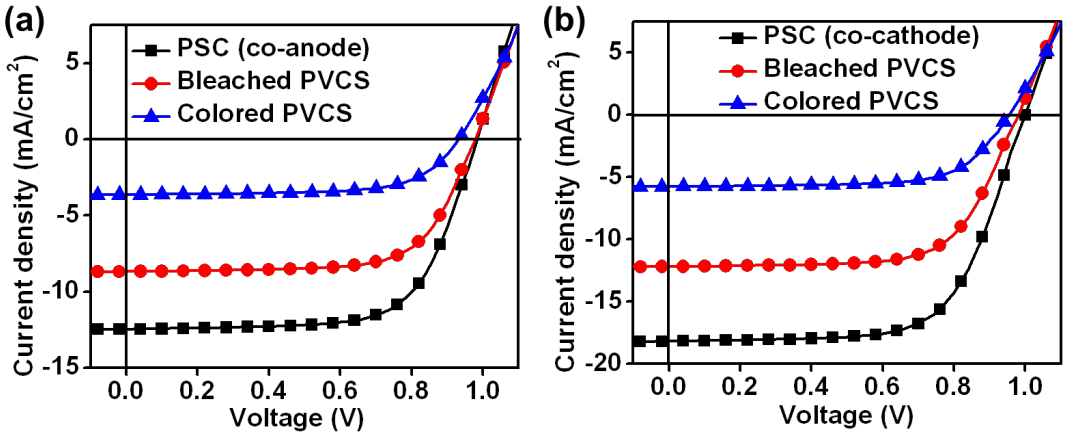

Figure 5. The photovoltaic performances of the PSCs utilizing in the two PVCSs before integration, the bleached PVCS, and the colored PVCS. The *J-V* curves of (a) co-anode PVCS and (b) co-cathode PVCS, respectively. The PSCs in the PVCSs is at a low-power working state under the colored state of the PVCSs.

Table 2. Lists of V_{oc}, J_{sc}, FF and PCE extracted from the *J-V* curves shown in the Figure 5(a) and 5(b).

Type	V_{oc} (V)	J_{sc} (mA/cm^2)	FF (%)	PCE (%)
Single PSC utilized in co-anode PVCS	0.983	12.46	67.3	8.25
Bleached co-anode PVCS	0.978	8.68	68.1	5.78
Colored co-anode PVCS	0.932	3.64	66.6	2.26
Single PSC utilized in co-cathode PVCS	1.000	18.17	65.4	11.89
Bleached co-cathode PVCS	0.981	12.18	66.8	7.98
Colored co-cathode PVCS	0.955	5.75	67.9	3.73

The low-power working state of PSC under the colored state of PVCSs also suggests an advantage of energy conservation in our device with extended lifetime. The color change of the ECS automatically switches off the solar light harvesting of the PSC and the photo-charging of the ECS, preventing the PSC from the long-time exposure under solar light, and slowing down the degradation of the PSC by blocking part of the solar light. Currently, the practical applications of the PSC are hindered by its stability, which can be resulted from ambient moisture or photo-degradation. [39-42] In view of this point, we conducted the photo-stability characterization of the as-fabricated PSC and our integrated co-cathode PVCS. Figure 6 shows the 4 normalized parameters (V_{oc}, J_{sc}, FF and PCE) as a function of the illumination time. We examined the photovoltaic performances of the PSC, bleached PVCS (to hold the device in a bleach stage, we disconnected the terminals A and C shown in the Figure 2 and keep the device in an open-circuit condition) and colored PVCS, which were continuously exposed to AM 1.5 G illumination for 5 hours. The PSC without the integration of ECS exposed directly to the solar light, and exhibited the most significant degradation, which is represented by its severe decreased J_{sc} and PCE to around 20% of their original values. The bleached PVCS shows a relatively slighter degradation, where the PCE is reduced to around 70% of the initial value after the continuous 5-hour photo-exposure. The photo-stability enhancement can mostly be attributed to that the bleached ECS selectively absorbs the part of the light and reflects the thermal radiation.[7, 8, 27] When the ECS is fully charged and turns to deep blue in the PVCSs, the PSC part is under a low-power working state and its lifetime is

prolonged. Once the ECS part is discharged and its color turns to be transparent, the PSC recovers to a working state.

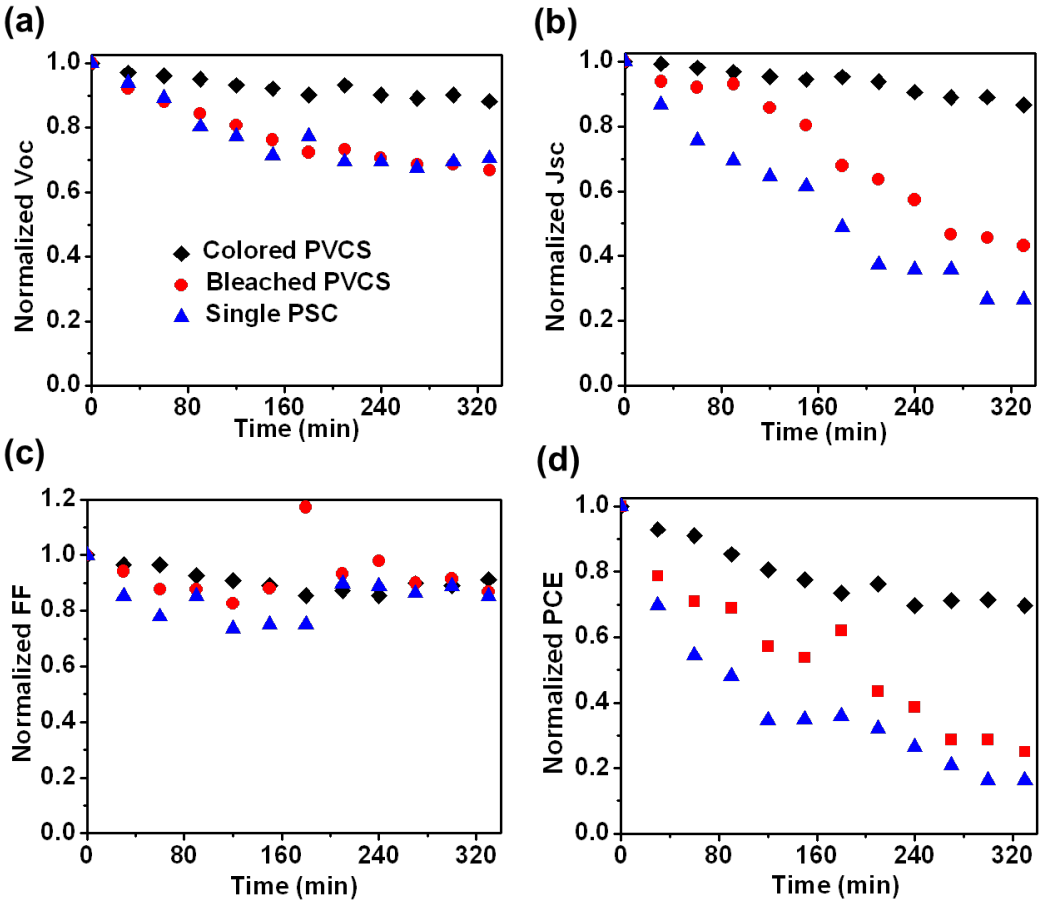

Figure 6. Photo-stability characterization of the as-fabricated PSC and the bleached/colored co-cathode PVCS during 5-hour continuous illumination: normalized 4 parameters (a) V_{oc}, (b) J_{sc}, (c) FF and (d) PCE as a function of the illumination time. The original values (0 min) of the 4 parameters are set as 1. The variations of the parameters with illumination time are normalized according to the values at 0 min.

Conclusions

In summary, we demonstrate co-anode and co-cathodes PVCSs integrating both semitransparent PSC and ECS. The PVCSs provide a seamless integration of energy harvesting and storage device, automatic and wide color tunability, and enhanced photo-stability of PSCs. The light power efficiency of the PV component in the

co-anode (co-cathode) PVCS is 8.25 (11.89) %. The energy density, power density and areal capacitance of the co-anode (co-cathode) PVCS are 13.4 (24.5) mWh/m^2, 187.6 (377.0) mW/m^2 and 286.8 (430.7) F/m^2, respectively. Accompanied with energy storage, the color of energy storage part ("electrochromic shelter" of PSC) changes from semitransparent to dark-blue with a reduction in AVT from 85% (76.2%) to 35.1% (23.0%) for co-anode (co-cathode) PVCS. As the colored PVCS blocks off most of the illuminated light, it automatically switches off the photo-charging. The PSC then works under a low-power operating state, which prevents the PSC from long-time photo-exposure and prolongs its lifetime. Our works provide great advantages over conventional smart window design.

Methods

Fabrication and Characterization of Perovskite Solar Cell. The patterned fluorine-doped tin oxide (FTO) coated glass substrates were cleaned with acetone, isopropanol and deionized water sequentially. The pre-cleaned substrates were then dried with nitrogen gas and further cleaned by UV-Ozone treatment. A solution prepared by mixing 1.25 ml acetic acid and titanium (IV) isopropoxide (TTIP) solution (1.25 ml) in anhydrous ethanol (15 ml) was spin coated (3500 rpm, 30 s) onto the cleaned substrates to from a compact titanium dioxide (c-TiO_2) layer. The prepared c-TiO_2 layer was then baked at 450 ºC for 2 hours in air. A one-step spin coating was applied to the deposition of perovskite layer ($CH_3NH_3PbI_{3-x}Cl_x$) in this work. The spin coating solution for the perovskite layer was prepared by mixing 2.4

M methylammonium iodide and 0.8 M lead chloride in N, N-dimethylformamide (DMF). The spin-coated perovskite thin film was then dried at 65 ℃ for 15 min and annealed at 105 ℃ for 45 min until the color turned to dark brown. To prepare the 2,2',7,7'-tetrakis(N,N-di-p-methoxyphenylamine)-9,9-spirobifluorene (spiro-MeOTAD) solution, 29 μl of 4-tert-butyl pyridine and 18 μl of lithium bis(trifluoromethanesulfonyl)imide (Li-TFSI) solution (520 mg Li-TFSI in 1 ml acetonitride, Sigma-Aldrich, 99.8%) was added into 953 μl of chlorobenzene dissolved with 80 mg spiro-MeOTAD powder. The solution was then spin coated on the perovskite layer at 4500 rpm for 30s. The prepared FTO/c-TiO2/$CH_3NH_3PbI_{3-x}Cl_x$/spiro-MeDTAD films were annealed in oxygen to enhance the cell performance. Finally, MoO3/Au/MoO3 electrodes (15 nm/ 12 nm/ 20 nm) were evaporated onto the devices, through which the device active area was defined as 0.06 cm^2. The solar source was provided by the Newport solar simulator (ORIEL Sol3ATM) and the electrical measurement was performed by B1500A semiconductor analyzer. The absorption spectra of perovskite film on quartz were examined using a UV-2550 Shimadzu UV-Vis spectrophotometer. X-ray diffraction (XRD) patterns of the perovskite film was determined by a Rigaku SmartLab X-ray diffractometer with a 2θ range from 10° to 70° in a step of 0.01°. Scanning electron microscopy (SEM) image was performed by Hitachi S-4800 field emission scanning electron microscope.

Fabrication and Characterization of Electrochromic Supercapacitor. A 300 nm-thick WO_3 thin film was thermally evaporated onto an FTO substrate as

supercapacitor electrode. The deposition was carried out with the background pressure of 5×10^{-6} Torr and the chamber pressure during the deposition was maintained at 3×10^{-5} Torr. The symmetric electrochromic supercapacitor was assembled by two identical WO_3 electrodes coated with the mixture of polyvinyl alcohol (PVA) and 1M H_2SO_4. Atomic force microscopy (AFM) image was examined by Bruker nanoscope 8. The electrochemical performances were characterized by electrochemical working station (CHI 660e, Shanghai Chenhua).

Integrated Device Characterization. The photo-charging process was performed under AM 1.5 illumination and the supercapacitor was discharged through electrochemical workstation. The transmittance spectra were obtained by using the UV-2550 Shimadzu UV-Vis spectrophotometer.

ACKNOWLEDGMENT

This work was supported in part by the Research Grant Council of Hong Kong (grant No.: PolyU 252001/14E); the National Natural Science Foundation of China (grant No. 61302045); the Hong Kong Polytechnic University (grant Nos: G-UC72, H-ZG1N, 1-BBA3, 1-ZVCG, and 4-BCAJ); F. Zhou and Prof. Y. Chai would like to acknowledge the supports by the University Research Facility in Materials Characterization and Device Fabrication of the Hong Kong Polytechnic University. Z. Ren and Prof. C. Surya acknowledge the supports from the RGC Theme-based Research Scheme (grant No.: HKU T23-713/11) and the Collaborative Research Grant (CUHK/CRF/12G) for the work conducted at the Hong Kong Polytechnic University. F. Zhou and Z. Ren contributed equally to this work.

ABBREVIATIONS

PVCS, photovoltachromic supercapacitor; PECC, photoelectrochromic; PVCC: photovoltachromic cell; DSSC, dye-sensitized solar cells; PSC, perovkiste solar cell; OPV, organic photovoltaics; CNT, carbon nanotube; AM 1.5, air mass 1.5; PCE, power conversion efficiency, ECS, electrochromic supercapacitor; CV, cyclic voltammetry; GCD, galvanostatic charging/discharging; FF, fill factor; $J_{sc,}$ short circuit current; $V_{oc,}$ open circuit voltage.

Supporting Information

Supporting Information Available: absorption and SEM image of perovskite film, *J-V* curve of PSC with Au top electrode, 3D schematics of co-anode and co-cathode PVCS, XPS spectra, SEM and AFM images of WO_3 film, ECS energy density and power density, capacitances of WO_3 ECS at different current densities, V-t curves of photo-charging and discharging processes of integrated ECS and PSC connected by external wires, *J-V* curve of a commercial Si solar cell and V-t curves of ECS charged by commercial solar cell. This material is available free of charge *via* the Internet at http://pubs.acs.org.

REFERENCES

1. Niklasson, G. A.; Granqvist, C. G., Electrochromics for Smart Windows: Thin Films of Tungsten Oxide and Nickel Oxide, and Devices Based on These. *J. Mater. Chem.* **2007,** *17*, 127-156.

2. Jaksic, N. I.; Salahifar, C., A Feasibility Study of Electrochromic Windows in

Vehicles. *Sol. Energy Mater. Sol. Cells* **2003,** *79*, 409-423.

3. Granqvist, C.-G.; Lansåker, P.; Mlyuka, N.; Niklasson, G.; Avendano, E., Progress in Chromogenics: New Results for Electrochromic and Thermochromic Materials and Devices. *Sol. Energy Mater. Sol. Cells* **2009,** *93*, 2032-2039.

4. Cannavale, A.; Fiorito, F.; Resta, D.; Gigli, G., Visual Comfort Assessment of Smart Photovoltachromic Windows. *Energy and Buildings* **2013,** *65*, 137-145.

5. Bechinger, C.; Ferrer, S.; Zaban, A.; Sprague, J.; Gregg, B. A., Photoelectrochromic Windows and Displays. *Nature* **1996,** *383*, 608-610.

6. Baetens, R.; Jelle, B. P.; Gustavsen, A., Properties, Requirements and Possibilities of Smart Windows for Dynamic Daylight and Solar Energy Control in Buildings: A State-of-The-Art Review. *Sol. Energy Mater. Sol. Cells* **2010,** *94*, 87-105.

7. Cannavale, A.; Eperon, G. E.; Cossari, P.; Abate, A.; Snaith, H. J.; Gigli, G., Perovskite Photovoltachromic Supercapacitors for Building Integration. *Energy Environ. Sci.* **2015,** *8*, 1578-1584.

8. Malara, F.; Cannavale, A.; Carallo, S.; Gigli, G., Smart Windows for Building Integration: A New Architecture for Photovoltachromic Devices. *ACS Appl. Mater. Interfaces* **2014,** *6*, 9290-9297.

9. Yang, M.-C.; Cho, H.-W.; Wu, J.-J., Fabrication of Stable Photovoltachromic Supercapacitors Using A Solvent-Free Hybrid Polymer Electrolyte. *Nanoscale* **2014,** *6*, 9541-9544.

10. Wu, J.-J.; Hsieh, M.-D.; Liao, W.-P.; Wu, W.-T.; Chen, J.-S., Fast-Switching Photovoltachromic Supercapacitors with Tunable Transmittance. *ACS Nano* **2009,** *3*, 2297-2303.

11. Xiao, X.; Li, T.; Yang, P.; Gao, Y.; Jin, H.; Ni, W.; Zhan, W.; Zhang, X.; Cao, Y.; Zhong, J., Fiber-Based All-Solid-State Flexible Supercapacitors for Self-Powered Systems. *ACS Nano* **2012,** *6*, 9200-9206.

12. Chen, T.; Qiu, L.; Yang, Z.; Cai, Z.; Ren, J.; Li, H.; Lin, H.; Sun, X.; Peng, H., An Integrated "Energy Wire" for Both Photoelectric Conversion and Energy Storage. *Angew. Chem., Int. Ed.* **2012,** *51*, 11977-11980.

13. Bae, J.; Park, Y. J.; Lee, M.; Cha, S. N.; Choi, Y. J.; Lee, C. S.; Kim, J. M.; Wang, Z. L., Single–Fiber–Based Hybridization of Energy Converters and Storage Units Using Graphene as Electrodes. *Adv. Mater.* **2011,** *23*, 3446-3449.

14. Wang, Q.; Chen, H.; McFarland, E.; Wang, L., Solar Rechargeable Batteries Based on Lead–Organohalide Electrolyte. *Adv. Energy Mater.* **2015,** *5*, 1501418.

15. Chien, C. T.; Hiralal, P.; Wang, D. Y.; Huang, I.; Chen, C. C.; Chen, C. W.; Amaratunga, G. A., Graphene−Based Integrated Photovoltaic Energy Harvesting/Storage Device. *Small* **2015,** *11*, 2929-2937.

16. Xu, J.; Chen, Y.; Dai, L., Efficiently Photo-Charging Lithium-Ion Battery by Perovskite Solar Cell. *Nat. Commun.* **2015,** *6,* 8103.

17. Xu, X.; Li, S.; Zhang, H.; Shen, Y.; Zakeeruddin, S. M.; Graetzel, M.; Cheng, Y.-B.; Wang, M., A Power Pack Based on Organometallic Perovskite Solar Cell and Supercapacitor. *ACS Nano* **2015,** *9*, 1782-1787.

18. Xie, Z.; Jin, X.; Chen, G.; Xu, J.; Chen, D.; Shen, G., Integrated Smart Electrochromic Windows for Energy Saving and Storage Applications. *Chem. Commun.* **2014,** *50*, 608-610.

19. Chen, X.; Sun, H.; Yang, Z.; Guan, G.; Zhang, Z.; Qiu, L.; Peng, H., A Novel "Energy Fiber" by Coaxially Integrating Dye-Sensitized Solar Cell and Electrochemical Capacitor. *J. Mater. Chem. A* **2014,** *2*, 1897-1902.

20. Dyer, A. L.; Bulloch, R. H.; Zhou, Y.; Kippelen, B.; Reynolds, J. R.; Zhang, F., A Vertically Integrated Solar−Powered Electrochromic Window for Energy Efficient Buildings. *Adv. Mater.* **2014,** *26*, 4895-4900.

21. Wang, K.; Wu, H.; Meng, Y.; Zhang, Y.; Wei, Z., Integrated Energy Storage and Electrochromic Function in One Flexible Device: An Energy Storage Smart Window. *Energy Environ. Sci.* **2012,** *5*, 8384-8389.

22. Wee, G.; Salim, T.; Lam, Y. M.; Mhaisalkar, S. G.; Srinivasan, M., Printable Photo-Supercapacitor Using Single-Walled Carbon Nanotubes. *Energy Environ. Sci.* **2011,** *4*, 413-416.

23. Yang, Z.; Li, L.; Luo, Y.; He, R.; Qiu, L.; Lin, H.; Peng, H., An Integrated Device for Both Photoelectric Conversion and Energy Storage Based on Free-Standing and Aligned Carbon Nanotube Film. *J. Mater. Chem. A* **2013,** *1*, 954-958.

24. Miyasaka, T.; Murakami, T. N., The Photocapacitor: An Efficient Self-Charging Capacitor For Direct Storage of Solar Energy. *Appl. Phys. Lett.* **2004,** *85*, 3932-3934.

25. Murakami, T. N.; Kawashima, N.; Miyasaka, T., A High-Voltage Dye-Sensitized Photocapacitor of A Three-Electrode System. *Chem. Commun.* **2005,** *26*, 3346-3348.

26. Ren, Z.; Ng, A.; Shen, Q.; Gokkaya, H. C.; Wang, J.; Yang, L.; Yiu, W.-K.; Bai, G.; Djurišić, A. B.; Leung, W. W.-f., Thermal Assisted Oxygen Annealing for High Efficiency Planar $CH_3NH_3PbI_3$ Perovskite Solar Cells. *Sci. Rep.* **2014,** *4,* 6752.

27. Xue, Z.; Liu, X.; Zhang, N.; Chen, H.; Zheng, X.; Wang, H.; Guo, X., High-Performance NiO/Ag/NiO Transparent Electrodes for Flexible Organic Photovoltaic cells. *ACS Appl. Mater. Interfaces* **2014,** *6*, 16403-16408.

28. Kim, K.-D.; Pfadler, T.; Zimmermann, E.; Feng, Y.; Dorman, J. A.; Weickert, J.; Schmidt-Mende, L., Decoupling Optical and Electronic Optimization of Organic Solar Cells Using High-Performance Temperature-Stable TiO_2/Ag/TiO_2 Electrodes. *APL Mater.* **2015,** *3*, 106105.

29. Hong, K.; Kim, K.; Kim, S.; Lee, I.; Cho, H.; Yoo, S.; Choi, H. W.; Lee, N.-Y.; Tak, Y.-H.; Lee, J.-L., Optical Properties of WO_3/Ag/WO_3 Multilayer as Transparent Cathode in Top-Emitting Organic Light Emitting Diodes. *J. Phys. Chem. C* **2011,** *115*, 3453-3459.

30. Yang, P.; Sun, P.; Chai, Z.; Huang, L.; Cai, X.; Tan, S.; Song, J.; Mai, W., Large−Scale Fabrication of Pseudocapacitive Glass Windows that Combine Electrochromism and Energy Storage. *Angew. Chem.* **2014,** *126*, 12129-12133.

31. Yang, P.; Sun, P.; Mai, W., Electrochromic Energy Storage Devices. *Mater. Today* **2015**. DOI: 10.1016/j.mattod.2015.11.007.

32. Yang, P.; Sun, P.; Du, L.; Liang, Z.; Xie, W.; Cai, X.; Huang, L.; Tan, S.; Mai, W., Quantitative Analysis of Charge Storage Process of Tungsten Oxide that Combines Pseudocapacitive and Electrochromic Properties. *J. Phys. Chem. C* **2015,** *119*, 16483-16489.

33. Chiang, K.-K.; Wu, J.-J., Fuel-Assisted Solution Route to Nanostructured Nickel Oxide Films for Electrochromic Device Application. *ACS Appl. Mater. Interfaces* **2013,** *5*, 6502-6507.

34. Hashimoto, S.; Matsuoka, H., Mechanism of Electrochromism for Amorphous WO_3 Thin Films. *J. Appl. Phys.* **1991,** *69*, 933-937.

35. Granqvist, C., Progress in Electrochromics: Tungsten Oxide Revisited. *Electrochim. Acta* **1999,** *44*, 3005-3015.

36. Song, R.; Jin, H.; Li, X.; Fei, L.; Zhao, Y.; Huang, H.; Chan, H. L.-W.; Wang, Y.; Chai, Y., A Rectification-Free Piezo-Supercapacitor with A Polyvinylidene Fluoride Separator and Functionalized Carbon Cloth Electrodes. *J. Mater. Chem. A* **2015,** *3*, 14963-14970.

37. Chen, J.; Yang, J.; Li, Z.; Fan, X.; Zi, Y.; Jing, Q.; Guo, H.; Wen, Z.; Pradel, K. C.; Niu, S., Networks of Triboelectric Nanogenerators for Harvesting Water Wave Energy: A Potential Approach Toward Blue Energy. *ACS Nano* **2015,** *9*, 3324-3331.

38. Xie, Y.; Liu, Y.; Zhao, Y.; Tsang, Y. H.; Lau, S. P.; Huang, H.; Chai, Y., Stretchable All-Solid-State Supercapacitor with Wavy Shaped Polyaniline/Graphene Electrode. *J. Mater. Chem. A* **2014,** *2*, 9142-9149.

39. Law, C.; Miseikis, L.; Dimitrov, S.; Shakya‐Tuladhar, P.; Li, X.; Barnes, P. R.; Durrant, J.; O'Regan, B. C., Performance and Stability of Lead Perovskite/TiO_2, Polymer/PCBM, and Dye Sensitized Solar Cells at Light Intensities up to 70 Suns. *Adv. Mater.* **2014,** *26*, 6268-6273.

40. Leijtens, T.; Eperon, G. E.; Pathak, S.; Abate, A.; Lee, M. M.; Snaith, H. J., Overcoming Ultraviolet Light Instability of Sensitized TiO_2 with Meso-Superstructured Organometal Tri-halide Perovskite Solar Cells. *Nat. Commun.* **2013,** *4,* 2885.

41. Ito, S.; Tanaka, S.; Manabe, K.; Nishino, H., Effects of Surface Blocking Layer of Sb_2S_3 on Nanocrystalline TiO_2 for $CH_3NH_3PbI_3$ Perovskite Solar Cells. *J. Phys. Chem. C* **2014,** *118*, 16995-17000.

42. Niu, G.; Guo, X.; Wang, L., Review of Recent Progress in Chemical Stability of Perovskite Solar Cells. *J. Mater. Chem. A* **2015,** *3*, 8970-8980.